DOI: 10.61782/fa.2025.0450

FORUM ACUSTICUM
EURONOISE 2025

IMPACT OF PHASE ANISOTROPY-RELATED SHIFTS ON THE CONTRAST OF DEFECT LOCALIZATION IMAGES IN REVERBERANT PLATES

Lynda Chehami* **Omar Bouchakour** **Emmanuel Moulin** **Elie Farha**

UPHF, CNRS, univ. Lille, UMR 8520-IEMN, F-59313, Valenciennes, France

ABSTRACT

Ultrasonic imaging based on beamforming relies generally on the precise synchronization of signals within a sensor network. Time shifts in these signals—often caused by sensor clock drifts—can be estimated and corrected during post-processing, prior to applying the backpropagation algorithm, using methods like the Peak Correlation Technique (PCT). However, in certain situations, particularly when defects exhibit anisotropy effects, additional time shifts can distort the backpropagated signals, undermining the accuracy of defect localization. This study focuses on statistically quantifying the impact of anisotropy-induced time shifts the contrast of defect localization images. The analysis is conducted in a thin reverberating plate, where covariance matrices are recorded in Full Matrix Capture (FMC) mode under two conditions: with and without a defect. Numerical simulations using A0 Lamb mode propagation are performed to validate the theoretical predictions.

Keywords: *Ultrasonic imaging, beamforming, Peak Correlation Technique, anisotropy-related shifts.*

1. INTRODUCTION

The demand for monitoring the structural integrity of infrastructures with minimal energy and hardware resources has led to the development of ”passive” imaging techniques. These methods leverage ambient noise to detect defects in reverberant media, eliminating the need for controlled emissions and ensuring substantial energy savings throughout the monitoring process. Studies such as [1, 2] have demonstrated that the Green’s function of a given medium can be reconstructed by cross-correlating ambient noise recordings from a network of sensors.

Structural Health Monitoring (SHM) has recently evolved with the increasing integration of autonomous sensor networks directly into infrastructures [3, 4]. This advancement revolutionizes integrity assessment by enabling continuous, real-time monitoring. Embedded sensors simplify traditional systems while enhancing efficiency, providing precise, instant data that supports swift, informed decisions, reducing failure risks and extending structural lifespan.

The use of autonomous sensor networks for SHM has significantly reduced costs and complexity, but signal resynchronization remains a major challenge. Each sensor relies on its own internal clock, leading to signal drift. Although various synchronization methods have been proposed, the most accurate ones require additional hardware, contradicting the goal of low-resource networks. The Peak Correlation Technique (PCT) [5–7] is a promising method for resynchronization, detecting time shifts by correlating the cross-correlation between signals. However, we have shown in previous works [8, 9] that noise in the measurement process can impair resynchronization and hinder defect localization.

In our previous studies, we assumed that the de-

*Corresponding author: lynda.chehami@uphf.fr.

fect scattered isotropically in all directions (constant scattering amplitude in all directions). However, in a more realistic scenario, the defect may exhibit preferred directions [10–12], which can also introduce shifts that overlap with resynchronization errors, further degrading the accuracy of defect localization. In this paper, we will conduct a statistical study of the shifts related to the anisotropy of the defect to quantify their impact on the contrast of defect localization images.

This work is structured as follows: we begin by theoretically quantifying the impact of shifts induced by defect anisotropy on its detection in elastic reverberating plates. Subsequently, we perform numerical simulations to validate the theoretical results.

2. THEORETICAL DEVELOPMENTS

We consider an array of N sensors placed on the surface of a plate subjected to ambient noise. As explained in [13], detecting a possible defect in a plate consists of calculating the cross-correlations between all pairs of sensors, both in the presence and absence of the defect, and then taking the difference to isolate the signature of the latter. We recall that for a pair n of sensors, in order to compensate for the propagation distance from the first sensor to the defect and then from the defect to the second sensor, we backpropagate the resynchronized differential cross-correlation in post-processing $\Delta C_n^{res+}(\omega)$ by multiplying it by a dispersion compensation term as follows:

$$BPF_n(\omega) = \Delta C_n^{res+}(\omega)\, e^{jk(\omega)d_n}, \tag{1}$$

with $BPF_n(\omega)$ the backpropagation of $\Delta C_n^{res+}(\omega)$ to the pixel corresponding to the position of the defect, $k(\omega)$ the wave number of the bending mode A_0 and d_n the sum of the distances from the first sensor to the defect and from the defect to the second sensor.

The inverse Fourier transform of $BPF_n(\omega)$ allows to find the backpropagated signals on the position of the defect in the time domain. We note that, these backpropagated signals correspond, ideally, to the autocorrelation of the emission signal. In the case of an isotropic defect, and if the signals are perfectly synchronized, the typical shape of these signals is as shown in Fig. 1. However, in the case of an anisotropic defect, the anisotropy influences both the amplitude and the phase of the backpropagated signals. As illustrated in Fig. 2, this results in time shifts and amplitude variations observable in the backpropagated signals.

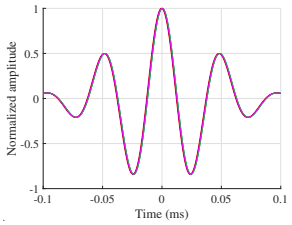

Figure 1. Example of back-propagated signals, on the defect position, in the case of an isotropic defect.

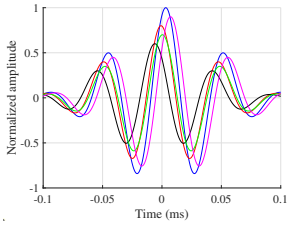

Figure 2. Example of back-propagated signals, on the defect position, in the case of an anisotropic defect ($\mathcal{E}_n = 0$ et $\tau_n \neq 0$).

In the remainder of this paper, we are interested in quantifying the contrast ratio defined in [8] as a function of the standard deviation of the initial shifts due to the phase anisotropy of the defect. To do this, we assume that back-propagated signals are affected both by the initial shifts and by the errors resulting from the imperfect resynchronization. As a result, the resynchronized version of the differential cross-correlation function becomes as follows:

$$\Delta C_n^{res+}(t) = \Delta C_n^{+}(t + \mathcal{E}_n + \tau_n), \tag{2}$$

with τ_n the initial shift due to the anisotropy of the defect and $\mathcal{E}_n$ the resynchronization error.

Which is equivalent, in the frequency domain, to:

$$\Delta C_n^{res+}(\omega) = \Delta C_n^{+}(\omega)\, e^{j\omega\mathcal{E}_n}\, e^{j\omega\tau_n}. \tag{3}$$

In a similar way to [8], we can express $\Delta C_n^{res+}(\omega)$ as follows:

$$\Delta C_n^{res+}(\omega) = f(\theta_n, \omega)\chi_n\, e^{-jk(\omega)d_n}\, U_0(\omega)\, e^{j\omega\mathcal{E}_n}\, e^{j\omega\tau_n}, \tag{4}$$

with $U_0(\omega)$ a term defined in [8].

Substituting Eq. 4 into Eq. 1 we obtain:

$$BPF_n(\omega) = f(\theta_n, \omega)\chi_n \, U_0(\omega) \, e^{j\omega\mathcal{E}_n} \, e^{j\omega\tau_n}. \quad (5)$$

Thus, the sum over the N_c pairs can be written as follows:

$$BPF(\omega) = \sum_{n=1}^{N_c} f(\theta_n, \omega)\chi_n \, U_0(\omega) \, e^{j\omega\mathcal{E}_n} \, e^{j\omega\tau_n}. \quad (6)$$

Returning to time domain and integrating the square of the modulus of $bpf(t)$, the inverse Fourier transform of $BPF(\omega)$, over an interval $[-T_0/2, T_0/2]$ containing the first wave packets, yields the intensity of the pixel corresponding to the defect position as follows:

$$I_{res} = \int_{-\frac{T_0}{2}}^{\frac{T_0}{2}} |bpf(t)|^2 \, \mathrm{d}t. \quad (7)$$

Replacing $bpf(t)$ with its expression (inverse Fourier transform of the Eq. 6) we obtain:

$$I_{res} = \int_{-\frac{T_0}{2}}^{\frac{T_0}{2}} \left(\sum_{n=1}^{N_c} f(\theta_n, \omega)\chi_n \tilde{u}_n(t) \right)^2 \mathrm{d}t, \quad (8)$$

with $\tilde{u}_n(t) = u_0(t + \mathcal{E}_n + \tau_n)$.

Similarly to [8], Eq. 8 becomes:

$$I_{res} = \frac{\sigma_0}{2\pi} \int_{-\frac{T_0}{2}}^{\frac{T_0}{2}} \left[\sum_{n=1}^{N_c} \chi_n^2 u_n^2 + \sum_{n=1}^{N_c} \sum_{m \neq n}^{N_c} \chi_n \chi_m \tilde{u}_n(t) \tilde{u}_m(t) \right] \mathrm{d}t. \quad (9)$$

Which can be written as follows :

$$I_{res} = \frac{\sigma_0}{2\pi} \left[E_0 \sum_{n=1}^{N_c} \chi_n^2 + \sum_{n=1}^{N_c} \sum_{m \neq n}^{N_c} \chi_n \chi_m \int_{-\frac{T_0}{2}}^{\frac{T_0}{2}} \tilde{u}_n(t) \tilde{u}_m(t) \, \mathrm{d}t \right]. \quad (10)$$

with $E_0 = \int_{-\frac{T_0}{2}}^{\frac{T_0}{2}} u_0^2(t) \, \mathrm{d}t$.

Since we are interested in an average behavior of the intensity on the position of the defect, we introduce the statistical average (denoted $\langle . \rangle$) on I_{res} for a set of random realizations on $\mathcal{E}_n$ and τ_n, and knowing that $\tilde{u}_n(t)$ and $\tilde{u}_m(t)$ are independent (because $\mathcal{E}_n$ and τ_n are assumed to be independent for $n \neq m$) we obtain:

$$\langle I_{res} \rangle = \frac{\sigma_0}{2\pi} \left(E_0 \sum_{n=1}^{N_c} \chi_n^2 + E_1 \sum_{n=1}^{N_c} \sum_{m \neq n}^{N_c} \chi_n \chi_m \right), \quad (11)$$

where $E_1 = \int_{-\frac{T_0}{2}}^{\frac{T_0}{2}} \langle \tilde{u}_n(t) \rangle^2 \, \mathrm{d}t$.

Then, Eq. 10 becomes:

$$\langle I_{res} \rangle = \frac{\sigma_0 N_c^2}{2\pi} \left[E_1 \, \bar{\chi}^2 + \frac{E_0 - E_1}{N_c} \bar{\chi^2} \right]. \quad (12)$$

Just like [8,9] , to quantify the degradation of the contrast ratio in the case of imperfect resynchronization, the definition of the contrast ratio consists of dividing the intensity of the Eq. 12 by a reference intensity calculated when the signals are perfectly resynchronized. This reference intensity can be expressed, by replacing E_1 with $E_0^{'}$ in the Eq. 12, as follows:

$$\langle I \rangle = \frac{\sigma_0 N_c^2}{2\pi} \left[E_0^{'} \, \bar{\chi}^2 + \frac{E_0 - E_0^{'}}{N_c} \bar{\chi^2} \right], \quad (13)$$

with $E_0^{'} = \int_{-\frac{T_0}{2}}^{\frac{T_0}{2}} \langle u_0(t + \tau_n) \rangle^2 \, \mathrm{d}t$.

Thus, under the assumption of a circular network around the defect, the contrast ratio defined in [8] can be written :

$$C_r = \frac{E_0 + (N_c - 1)E_1}{E_0 + (N_c - 1)E_0^{'}}. \quad (14)$$

Using Parseval's theorem and the transfer theorem in the same way as in [8], we can show that E_1 can be written:

$$E_1 = 4\pi^2 \int |U_0(\omega)|^2 \, |p_{\mathcal{E}}(\omega)|^2 \, |p_\tau(\omega)|^2 \, \mathrm{d}\omega, \quad (15)$$

with $p_{\mathcal{E}}(\omega)$ and $p_\tau(\omega)$ are the Fourier transforms of the probability density of the resynchronization errors and that of the initial shifts, respectively.

Similarly, we can easily show that:

$$E_0^{'} = 2\pi \int |U_0(\omega)|^2 \, |p_\tau(\omega)|^2 \, \mathrm{d}\omega. \quad (16)$$

As for E_0, its expression can be found in [8].

Finally, the Eq. 14 becomes:

$$C_r = \frac{\int |U_0(\omega)|^2 \, \mathrm{d}\omega + 4\pi^2 (N_c - 1) \int |U_0(\omega)|^2 |p_{\mathcal{E}}(\omega)|^2 |p_\tau(\omega)|^2 \, \mathrm{d}\omega}{\int |U_0(\omega)|^2 \, \mathrm{d}\omega + 2\pi (N_c - 1) \int |U_0(\omega)|^2 |p_\tau(\omega)|^2 \, \mathrm{d}\omega}. \tag{17}$$

This expression, which generalizes the expression developed in [8] for the case where the defect is anisotropic, shows that resynchronization errors affect the numerator of the contrast ratio, while initial shifts influence both the numerator and the denominator of this ratio. We will explore and confirm this relationship through a numerical simulation in the next section.

3. NUMERICAL VALIDATION

To validate the theoretical results obtained in the previous section, a numerical simulation is performed here using a finite element code ELMER. This code models acoustic wave propagation in a finite plate based on the Reissner-Mindlin plate theory.

The configuration tested (see Fig. 3) consists of an aluminum plate of dimensions 1×0.5 m^2 and thickness 3 mm. On the surface of this plate, we place an array of 8 sensors at known positions and a distribution of 600 sources uniformly distributed around the sensors. A defect is modeled by a zero normal displacement imposed at the position (53, 26) cm on the surface of the plate.

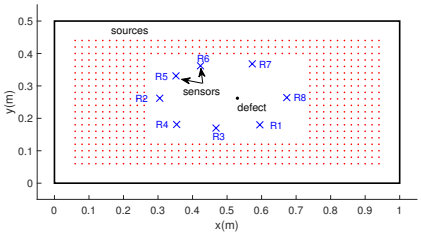

Figure 3. Simulated configuration: aluminum plate 1×0.5 m^2 and 3 mm thick. 8 sensors (blue crosses). 600 sources uniformly distributed around the sensors (red dots). A point defect at position (53, 26) cm.

The emission signal is a Gaussian-windowed sine of frequency $f_0 = 20$ kHz. The sampling frequency is 2.5 MS/s. For each pair of receivers, the summed cross-correlation over all sources is computed.

We whiten the simulated signals between 1 kHz and 30 kHz and then calculate the cross-correlations for all sensor pairs in the cases with and without defects. Next, we introduce initial shifts according to a Gaussian distribution with zero mean and variable standard deviation, denoted σ_τ. For each value of σ_τ, we add to these cross-correlations resynchronization errors modeled by a normal distribution with zero mean and variable standard deviation σ. We then apply the localization algorithm [13] to the obtained cross-correlations. Finally, we calculate the contrast ratio averaged over 100 draws of the initial shifts and 100 draws of the resynchronization errors. This numerical contrast ratio can be compared to the theoretical curve of the Eq. 17.

The curves showing the evolution of the contrast ratio as a function of σ for different values of σ_τ are shown in Fig. 4.

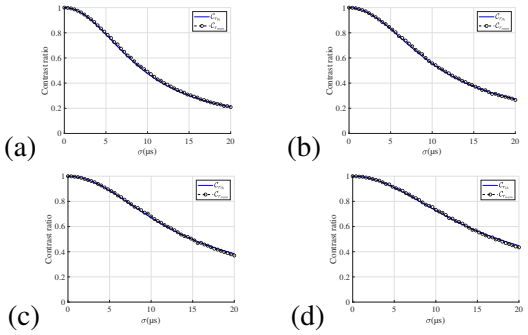

Figure 4. Comparison between the variation of the theoretical (blue line) and numerical (black circles) contrast ratio, as a function of σ, the standard deviation of the resynchronization errors, for different values of the standard deviation of the initial shifts : (a) $\sigma_\tau = 2$ µs, (b) $\sigma_\tau = 6$ µs, (c) $\sigma_\tau = 10$ µs, (d) $\sigma_\tau = 12$ µs.

On the one hand, we observe that the numerical results are in excellent agreement with the theory. On the other hand, it is clear that an increase in σ_τ causes a significant change in the shape of the curves.

4. CONCLUSION

In this paper, we have explored the impact of defect scattering anisotropy on the signals used for localization. We demonstrated that phase anisotropy leads to initial shifts in

the signals. These shifts can overlap with resynchronization errors and significantly affect the contrast in defect localization images. In future works, the results presented in this paper could be used to classify defects by conducting a detailed analysis of the initial shifts. This classification could be further refined by incorporating the defect's scattering cross section into the contrast ratio calculation.

5. REFERENCES

[1] O. I. Lobkis and R. L. Weaver, "On the emergence of the Green's function in the correlations of a diffuse field," *J. Acoust. Soc. Am.*, vol. **110**, pp. 3011–3017, 2001.

[2] A. Colombi, L. Boschi, P. Roux, and M. Campillo, "Green's function retrieval through cross-correlations in a two-dimensional complex reverberating medium," *J. Acoust. Soc. Am.*, vol. **135**, no. 3, pp. 1034–1043, 2014.

[3] T. Buckley, B. Ghosh, and V. Pakrashi, "Edge structural health monitoring (e-shm) using low-power wireless sensing," *Sensors*, vol. 21, no. 20, p. 6760, 2021.

[4] A. Sofi, J. Regita, B. Rane, and H. H. Lau, "Structural health monitoring using wireless smart sensor network–an overview," *Mech. Syst. Signal Process.*, vol. 163, p. 108113, 2022.

[5] K. G. Sabra, P. Roux, A. M. Thode, G. L. D'Spain, W. Hodgkiss, and W. Kuperman, "Using ocean ambient noise for array self-localization and self-synchronization," *IEEE Journal of Oceanic Engineering*, vol. **30**, no. 2, pp. 338–347, 2005.

[6] C. Sens-Schönfelder, "Synchronizing seismic networks with ambient noise," *Geophys. J. Int.*, vol. **174**, no. 3, pp. 966–970, 2008.

[7] L. Tenorio-Hallé, A. M. Thode, S. L. Swartz, and J. U. R, "Using anisotropic and narrowband ambient noise for continuous measurements of relative clock drift between independent acoustic recorders," *J. Acoust. Soc. Am.*, vol. **149**, no. 6, pp. 4094–4105, 2021.

[8] O. Bouchakour, E. Moulin, L. Chehami, and N. Smagin, "Quantification and mitigation of the effect of resynchronization errors in ultrasound sensor network for passive imaging in elastic plates," *J. Acoust. Soc. Am.*, vol. **155**, no. 5, pp. 3283–3290, 2024.

[9] O. Bouchakour, E. Moulin, and L. Chehami, "Impact of resynchronization errors on the localization quality of defects in reverberant plates," in *Journal of Physics: Conference Series*, vol. **2904**, p. 012006, IOP Publishing, 2024.

[10] U. Cicekli, G. Z. Voyiadjis, and R. K. A. Al-Rub, "A plasticity and anisotropic damage model for plain concrete," *Int. J. Plast.*, vol. **23**, no. 10-11, pp. 1874–1900, 2007.

[11] T. R. Jebieshia, D. K. Maiti, and D. Maity, "Vibration characteristics and damage detection of composite structures with anisotropic damage using unified particle swarm optimization technique," in *Proceedings of the American Society for Composites, 13th Technical Conference, Michigan State University, East Lansing, MI*, pp. 28–30, 2015.

[12] R. Desmorat, "Anisotropic damage modeling of concrete materials," *Int. J. Damage Mech.*, vol. **25**, no. 6, pp. 818–852, 2016.

[13] L. Chehami, E. Moulin, J. de Rosny, C. Prada, O. B. Matar, F. Benmeddour, and J. Assaad, "Detection and localization of a defect in a reverberant plate using acoustic field correlation," *J. Appl. Phys.*, vol. **115**, no. 10, p. 104901, 2014.